

FRÉCHET MEANS OF CURVES FOR SIGNAL AVERAGING AND APPLICATION TO ECG DATA ANALYSIS

BY JÉRÉMIE BIGOT

DMIA - ISAE

Signal averaging is the process that consists in computing a mean shape from a set of noisy signals. In the presence of geometric variability in time in the data, the usual Euclidean mean of the raw data yields a mean pattern that does not reflect the typical shape of the observed signals. In this setting, it is necessary to use alignment techniques for a precise synchronization of the signals, and then to average the aligned data to obtain a consistent mean shape. In this paper, we study the numerical performances of Fréchet means of curves which are extensions of the usual Euclidean mean to spaces endowed with non-Euclidean metrics. This yields a new algorithm for signal averaging and for the estimation of the time variability of a set of signals. We apply this approach to the analysis of heart beats from ECG records.

1. Introduction. In many applications (biology, medicine, road traffic data) one observes a set of signals that have a similar shape. This may lead to the assumption that such observations are random elements which vary around the same but unknown mean shape. Signal averaging is then the process that consists in computing a mean curve which reflects the typical shape of the observed signals. This procedure generally amounts to find an appropriate combination of the data to compute an average shape with a better signal-to-noise ratio. In many situations, the observed signals exhibit not only a classical source of random variation in amplitude, but also a less standard source of variability in time. Due to this source of time variability, the usual Euclidean mean of the raw data may yield a mean curve that does not reflect the typical shape of the signals, as illustrated by the following application.

1.1. *Signal averaging in ECG data analysis.* An important application of signal averaging is the estimation of a mean heart cycle from electrocardiogram (ECG) records. An ECG signal corresponds to the recording of the

AMS 2000 subject classifications: Primary 62G08; secondary 62P10

Keywords and phrases: Signal averaging, Mean shape, Fréchet means, Curve registration, Geometric variability, Deformable models, ECG data

heart electrical activity. It is a signal, recorded over time, that is composed of the succession of cycles of contraction and release of the heart muscle. Each recorded cycle is a curve composed of a characteristic P-wave, reflecting the atrial depolarization, that is followed by the so-called QRS complex which corresponds to the depolarization of the ventricles, and which ends with a T-wave reflecting the repolarization of the heart. The QRS complex refers to the succession of the Q wave (a downward deflection), the R wave (an upward deflection), and the S wave (a downward deflection). The shape of the combination of these three successive waves is useful for the diagnosis of cardiac pathologies such as arrhythmia. For a more precise description of an ECG recording we refer to [Guyton and Hall \(2006\)](#). In this paper, we present results on data sets from the QT database [Goldberger *et al.* \(2000\)](#) (in ECG analysis, the QT interval corresponds to the time between the beginning of the Q wave and the end of the T wave in a heart cycle). In [Figure 1](#), we display data from an ECG record of a subject showing evidence of significant arrhythmia (note that, in all the figures showing ECG data, units on the vertical axis are in millivolts).

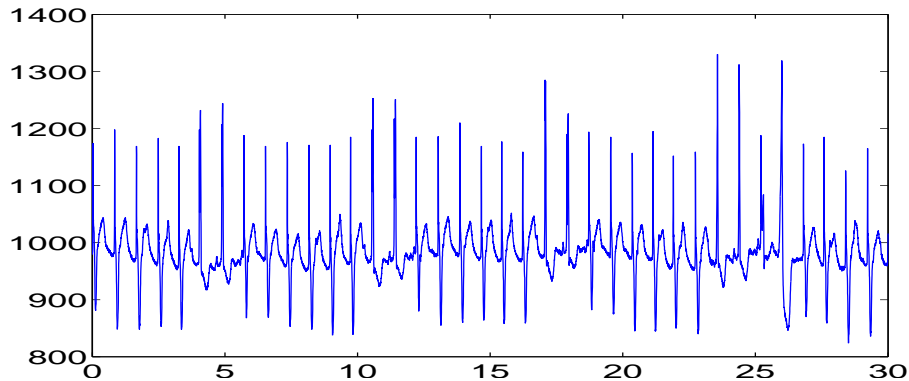


FIG 1. ECG recording of a subject showing evidence of significant arrhythmia (30 first seconds of patient *Sel104* from the QT database).

In the analysis of ECG data, it is generally assumed that the heart electrical activity repeats itself. Therefore, during an ECG record, one classically considers that the heart cycle of interest remains approximately the same with every beat, and that it is embedded in a random noise with zero expectation that is uncorrelated with the mean shape to be estimated. After an appropriate segmentation of an ECG record, one observes a set of signals of the same length such that each of them contains a single QRS complex. The preliminary segmentation step is done by taking segments (of the same

length) in the ECG record that are centered around the easily detectable maxima of the QRS complex of the beats. Identification of these maxima can be done using statistical methods to identify local extrema in noisy signals Bigot (2006); Gasser and Kneip (1995) or by applying appropriate digital filters to identify typical parts of the QRS complex Pan and Tompkins (1985). In this paper, we used the approach in Bigot (2006) to identify local maxima and to segment an ECG record into signals of the same length containing a single QRS complex. In this segmentation of the long ECG record displayed in Figure 1, we have only extracted non-overlapping segments. Therefore, some parts of the original signal, that do not contain significant peaks corresponding to the QRS complex, have been discarded from the statistical analysis. After this preliminary segmentation, one thus observes signals with approximately the same shape. For the patient Sel104 from the QT database, we obtained $J = 285$ signals (from a 4-minutes record) of length $n = 128$ time points. Four of these signals containing a single QRS complex are displayed in Figure 2.

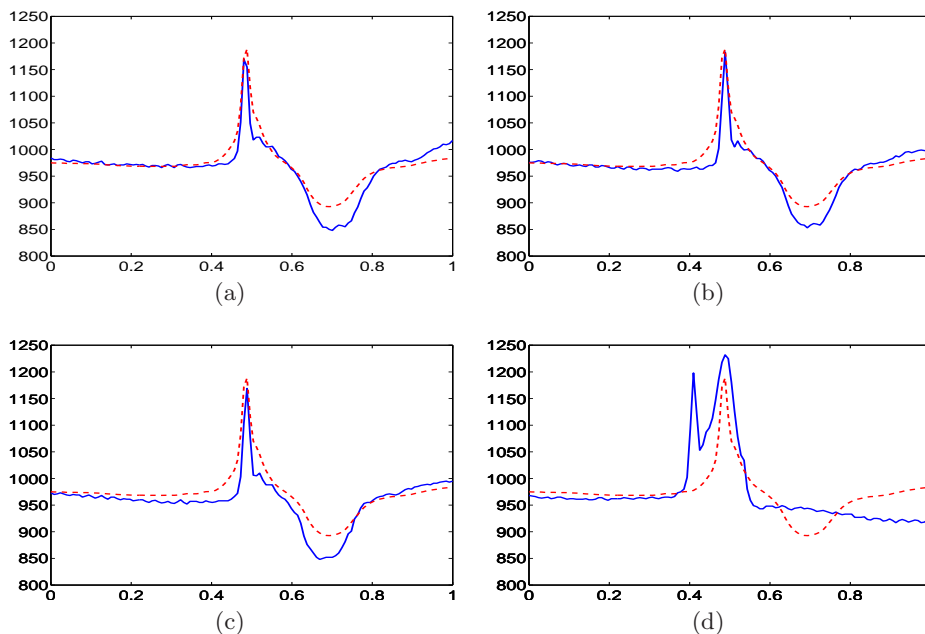


FIG 2. Patient Sel104 - case of cardiac arrhythmia. Solid and blue curves: four signals containing a single QRS complex out of $J = 285$ extracted from the ECG recording displayed in Figure 1. The length of the signals is $n = 128$ time points. Dashed and red curve: Euclidean mean of the raw data. Units on the horizontal axis are arbitrary.

To estimate the typical shape of a heart cycle and to improve the signal-to-noise ratio, one may use the Euclidean mean of these signals. In the case of a normal ECG record from a healthy subject, this generally leads to satisfactory results as this average signal clearly reflects the typical shape of the observed heart beats. However, in the case of cardiac arrhythmia, the electrical activity of the heart is more irregular. This can be seen in the shape of the heart beats displayed in Figure 2 which may vary significantly from one pulse to another. Due to noise and time variability in the measurements, a simple averaging step may cause a low-pass filtering effect that leads to a mean cycle that does not reflect the typical shape of the heart beats in the ECG record, see *e.g.* Laciár, Jané and Brooks (2003); Rompelman and Ros (1986a,b). In Figure 2, we have superposed the Euclidean mean (red dashed curve) on the four heart beats. One can see that averaging the raw data causes a low-pass filtering effect in the shape of the QRS complex, as shown by the shape of the Euclidean mean displayed in Figure 2. Indeed, around the time point $t_0 \approx 0.45$ (which corresponds to the beginning of the QRS complex), in the shape of the observed heart beats, there is rapid transition between a flat region and the peak of the R wave. The Euclidean mean has clearly a different shape around $t_0 \approx 0.45$ since this transition is slower. More precisely, the Euclidean mean is a local convolution by a smooth kernel of the heart beats around the time point $t_0 \approx 0.45$. To interpret this local convolution, assume that one observes J signals denoted by f_1, \dots, f_J obtained by random deformations around the time t of a reference signal f , namely

$$f_j(t_0) = f(t_0 - \theta_j), \quad j = 1, \dots, J,$$

where the θ_j 's are i.i.d. random variables sampled from a density g . These random translations of f model a local source of time variability in the data around t_0 . Under mild conditions, the Euclidean mean of the f_j 's is not a consistent estimator of f a time t_0 since

$$\bar{f}_J(t_0) = \frac{1}{J} \sum_{j=1}^J f_j(t_0) \rightarrow \int f(t_0 - \theta)g(\theta)d\theta, \quad \text{a.s. as } J \rightarrow +\infty,$$

showing that \bar{f}_J rather converges to the convolution of f by the density g .

To obtain better results, it is necessary to use alignment techniques for a precise synchronization of the heart beats. In this paper, we develop an algorithm that is composed of the following key steps:

(a) we initially smooth each observed curve in the data using standard techniques from nonparametric regression (*e.g.* Fourier filtering or wavelet thresholding),

(b) we consider deformation operators depending on finite-dimensional parameters to model time variability in the data,

(c) we define a mean signal by minimizing an objective function that is inspired by the notion of Fréchet mean, and which results in finding appropriate time deformations for an optimal synchronization of the smoothed curves, see equation (1.2) below.

1.2. *A deformable model.* Assume for simplicity that the signals are observed on the time interval $[0, 1]$, and that they can be extended outside $[0, 1]$ (e.g. by periodicity). An alignment technique consists in finding a time synchronization of a set of signals. To be more precise, define a deformation operator $\phi_{\boldsymbol{\theta}}$ parametrized by $\boldsymbol{\theta} \in \mathbb{R}^p$ as a smooth increasing function $\phi_{\boldsymbol{\theta}} : [0, 1] \rightarrow \mathbb{R}$ such that

$$\phi_{\boldsymbol{\theta}}^{-1}(t) = \phi_{-\boldsymbol{\theta}}(t) \text{ for all } t \in [0, 1].$$

In the paper, we shall consider the following families of deformation operators:

- *Translation operators:* $\phi_{\boldsymbol{\theta}}(t) = t - \boldsymbol{\theta}$ and $\phi_{\boldsymbol{\theta}}^{-1}(t) = \phi_{-\boldsymbol{\theta}}(t) = t + \boldsymbol{\theta}$, for $\boldsymbol{\theta} \in \mathbb{R}$ ($p = 1$) and all $t \in [0, 1]$.
- *Non-rigid operators:* $\phi_{\boldsymbol{\theta}} : [0, 1] \rightarrow [0, 1]$ is diffeomorphism of $[0, 1]$ parametrized by some $\boldsymbol{\theta} \in \mathbb{R}^p$, i.e. a smooth increasing function with $\phi_{\boldsymbol{\theta}}(0) = 0$ and $\phi_{\boldsymbol{\theta}}(1) = 1$ (a general method for constructing non-rigid deformation operators is described in Section 2.2).

Given $f_1, f_2 : [0, 1] \rightarrow \mathbb{R}$ and a family $(\phi_{\boldsymbol{\theta}})_{\boldsymbol{\theta} \in \mathbb{R}^p}$ of deformation operators, the problem of time synchronization of two signals is to find a $\boldsymbol{\theta} \in \mathbb{R}^p$ such $f_1(\phi_{\boldsymbol{\theta}}(t)) \approx f_2(t)$ for all $t \in [0, 1]$. In ECG data analysis, the most widely used alignment technique is time synchronization using translation operators by temporal or multiscale cross-correlation, see [Laciar, Jané and Brooks \(2003\)](#); [Trigano, Isserles and Ritov \(2011\)](#) and references therein.

In the presence of time variability in the data, it is reasonable to assume that the signals at hand satisfy the following deformable (or perturbation) model:

$$(1.1) \quad Y_j^\ell = f(\phi_{\boldsymbol{\theta}_j^*}(t_\ell)) + w_j^\ell, \quad j = 1, \dots, J, \quad \text{and } \ell = 1, \dots, n,$$

where Y_j^ℓ denotes the ℓ -th observation for the j -th signal and $t_\ell = \frac{\ell}{n}$ are equi-spaced design points in $[0, 1]$. The function $f : [0, 1] \rightarrow \mathbb{R}$ in model (1.1) is the unknown mean shape of the signals. The w_j^ℓ are supposed to be random variables with zero expectation that represent additive noise in the measurements. Finally, the $\boldsymbol{\theta}_j^*$'s are assumed to be i.i.d. random variables

in \mathbb{R}^p with zero expectation, and the random deformation operators $\phi_{\theta_j^*}$ represent time variability in the data.

In the simplest case, where the w_j^ℓ 's are i.i.d. normal variables with zero expectation and variance σ_j^2 , then (1.1) corresponds to the so-called shape invariant model (SIM) that has received a lot of attention in the statistical literature, see *e.g.* Bigot and Charlier (2011), Kneip and Gasser (1988) and references therein.

The deformable model (1.1) is well adapted to ECG data processing. The main type of perturbations related to the analysis of ECG data (see *e.g.* Laciár, Jané and Brooks (2003); Trigano, Isserles and Ritov (2011)) are the baseline wandering effect (a low-frequency signal), electromyographic (EMG) noise, and power-line interference which is an amplitude and frequency varying sinusoid. This source of additive noise can be modeled in (1.1) by the random variables w_j^ℓ which represent (possibly smooth) variations in the data around the mean shape f . The physiological nature of the electrocardiographic signal also alters the recording from heartbeat to heartbeat in lag and duration. In the ECG signal, there are therefore variations in time of the heart cycle from one beat to another. This makes the heartbeats look shorter or longer in duration. After the segmentation of an ECG record into signals containing a single QRS complex, this local variability in time is modeled in (1.1) by the non-rigid deformation operators $\phi_{\theta_j^*}$. Aligning heart beats using non-rigid deformation operators is an alternative to the cross-correlation method which is classical used in ECG data analysis.

1.3. *Fréchet means of curves.* The problem of estimating f and the deformation parameters θ_j^* in the deformable model (1.1) has been studied in Bigot and Charlier (2011); Bigot and Gendre (2013) using the following procedure. First, for each $j = 1, \dots, J$, smooth the data $(Y_j^\ell)_{\ell=1}^n$ to construct an estimator $\hat{f}_j : [0, 1] \rightarrow \mathbb{R}$ of $f \circ \phi_{\theta_j^*}$. In this paper, this smoothing step is done either by low-pass Fourier filtering or by wavelet thresholding. In a second step, estimate simultaneously the deformation parameters $\theta_j^*, j = 1, \dots, J$ by minimizing the following criterion

$$(1.2) \quad (\hat{\theta}_1, \dots, \hat{\theta}_J) = \underset{(\theta_1, \dots, \theta_J) \in \Theta_0}{\operatorname{argmin}} M(\theta_1, \dots, \theta_J),$$

where

$$(1.3) \quad M(\theta_1, \dots, \theta_J) = \frac{1}{J} \sum_{j=1}^J \frac{1}{n} \sum_{\ell=1}^n \left(\hat{f}_j(\phi_{-\theta_j}(t_\ell)) - \frac{1}{J} \sum_{j'=1}^J \hat{f}_{j'}(\phi_{-\theta_{j'}}(t_\ell)) \right)^2,$$

and

$$\Theta_0 = \{(\theta_1, \dots, \theta_J) \in (\mathbb{R}^p)^J, \theta_1 + \dots + \theta_J = 0\}.$$

Finally, in a third step take

$$(1.4) \quad \hat{f}(t) = \frac{1}{J} \sum_{j=1}^J \hat{f}_j(\phi_{-\hat{\theta}_j}(t)),$$

as an estimator of the mean shape f .

As explained in [Bigot and Charlier \(2011\)](#); [Bigot and Gendre \(2013\)](#), the estimator \hat{f} can be interpreted as a smoothed Fréchet mean of the observed signals. The Fréchet mean [Fréchet \(1948\)](#) is an extension of the usual Euclidean mean to spaces endowed with non-Euclidean metrics. We refer to [Afsari \(2011\)](#) and [Huckemann \(2011\)](#) for recent overviews of this notion and its application to the analysis of random variables taking their values in non-linear manifolds.

The constrained set Θ_0 (onto which the minimization of $M(\theta_1, \dots, \theta_J)$ is done) reflects the assumption that the deformation parameters θ_j^* in model (1.1) have zero expectation. The choice of this constraint is also related to identifiability issues in model (1.1), and we refer to [Bigot and Charlier \(2011\)](#) for a detailed discussion on that point.

In [Bigot and Charlier \(2011\)](#); [Bigot and Gendre \(2013\)](#), the statistical properties of \hat{f} and the $\hat{\theta}_j$'s in deformable models such as (1.1), have been studied in details in the asymptotic setting $n \rightarrow +\infty$ and/or $J \rightarrow +\infty$. However, in these papers, the benefits of Fréchet means for the analysis of real data such as ECG records has not been considered.

1.4. *Previous work on signal averaging.* In statistics, the problem of estimating the mean shape of a set of curves that differ by a time transformation is usually referred to as the curve registration problem. It has received a lot of attention in the statistical literature over the last two decades, and for further details we refer to [Bigot \(2006\)](#), [Ramsay and Li \(2001\)](#), [Wang and Gasser \(1997\)](#), [Liu and Muller \(2004\)](#), [Kneip and Gasser \(1988\)](#), [Trigano, Isserles and Ritov \(2011\)](#).

Our approach also share various similarities with Procrustes methods that were originally developed for the analysis of planar shapes. In particular, the full Procrustes mean of shapes described by landmarks in \mathbb{R}^2 is defined through a Fréchet-type objective function such as (1.3), see *e.g.* [Goodall \(1991\)](#). In the case of curve registration, the term Procrustes has also been attached to methods of time warping although the settings of curve alignment and planar shape analysis are clearly different.

In the statistical literature, the criterion (1.2) has been first proposed by [Gamboa, Loubes and Maza \(2007\)](#) in the case of translation operators and then further studied by [Vimond \(2010\)](#), [Bigot and Gadat \(2010\)](#). Its

generalization to other deformation operators and the connection between minimizing (1.3) and the computation of Fréchet means of curves has been investigated in Bigot and Charlier (2011); Bigot and Gendre (2013). Note that various theoretical arguments are given in Bigot and Charlier (2011); Bigot and Gadat (2010); Bigot and Gendre (2013) to show that, without a pre-smoothing step, the Fréchet mean cannot be consistent. Note that in curve registration or Procrustes methods, one generally registers the raw data without any preliminary smoothing. One the purposes of this paper is thus to show that it is preferable to first smooth the data before alignment.

The method that we propose is not the only shape averaging algorithm in the literature. In particular, for the statistical analysis of images or surfaces, there exist several methods based on different alignment techniques though the use of deformations operators, see *e.g.* Allasonnière, Amit and Trounev (2007) and Ma *et al.* (2008) for a Bayesian approach to compute a mean pattern from two-dimensional images, Klassen *et al.* (2004) and Fletcher *et al.* (2004) for the statistical analysis of shapes using geodesic paths and Riemannian geometry.

1.5. *Organization of the paper.* In Section 2 we describe more precisely the smoothed Fréchet mean in the case of translation and non-rigid operators. We also use some numerical experiments to illustrate the advantages of a pre-smoothing step before alignment. The usefulness of the Fréchet mean for signal averaging and for the estimation of time variability in ECG data analysis is presented in Section 3. We conclude the paper by a brief discussion on these results and the benefits of our approach.

2. Methodology for mean pattern estimation.

2.1. *Choice of the regularization parameter in the smoothing step.* For the smoothing step, we present numerical results for:

- *low-pass Fourier filtering:* for $t \in [0, 1]$

$$\hat{f}_j(t) = \sum_{|k| \leq \hat{\lambda}_j} c_k^{(j)} e^{i2\pi kt},$$

with $c_k^{(j)} = \frac{1}{n} \sum_{\ell=1}^n Y_{j,\ell} e^{-i2\pi k \frac{\ell}{n}}$, and where $\hat{\lambda}_j \in \mathbb{N}$ is a regularization parameter (cut-off frequency). A possible data-based choice for $\hat{\lambda}_j$ is to use generalized cross validation (GCV), see *e.g.* Craven and Wahba (1979).

- *wavelet smoothing by hard thresholding*: for $t \in [0, 1]$

$$\hat{f}_j(t) = \sum_{k=0}^{2^{m_0}} \alpha_{m_0,k}^{(j)} \phi_{m_0,k}(t) + \sum_{m=m_0}^{m_1} \sum_{k=0}^{2^m} \beta_{m,k}^{(j)} \mathbb{1}_{\{|\beta_{m,k}^{(j)}| \geq \hat{\sigma}_j \sqrt{2 \log(n)}\}} \psi_{m,k}(t),$$

where $\phi_{m_0,k}(t) = 2^{\frac{m_0}{2}} \phi(2^{m_0}t - k)$ and $\psi_{m,k}(t) = 2^{\frac{m}{2}} \psi(2^m t - k)$ are the usual scaling and wavelet basis functions at resolution levels $0 \leq m_0 \leq m \leq m_1$ and location k , $\alpha_{m_0,k}^{(j)}, \beta_{m,k}^{(j)}$ are respectively the empirical scaling and wavelet coefficients computed from the data $(Y_j^\ell)_{\ell=1}^n$ (for further details on wavelet thresholding see *e.g.* [Antoniadis, Bigot and Sapatinas \(2001\)](#)). The universal threshold $\hat{\sigma}_j \sqrt{2 \log(n)}$ depends on the estimation $\hat{\sigma}_j$ of the level of noise in the j -th signal. It is given by the median absolute deviation (MAD) of the empirical wavelet coefficients at the highest level of resolution m_1 (see *e.g.* [Antoniadis, Bigot and Sapatinas \(2001\)](#)).

2.2. *The case of non-rigid operators.* To build a family $(\phi_\theta)_{\theta \in \mathbb{R}^p}$ of parametric diffeomorphisms of $[0, 1]$, we adapt to one-dimensional curves the approach proposed in [Bigot, Gadat and Loubes \(2009\)](#) to compute the mean pattern of a set of two-dimensional images. Let $v : [0, 1] \rightarrow \mathbb{R}$ be a smooth parametric vector field given by a linear combination of p basis functions $\{h_k : [0, 1] \rightarrow \mathbb{R}, k = 1, \dots, p\}$, such that

$$v(t) = \sum_{k=1}^p \theta_k h_k(t) \text{ for } t \in [0, 1],$$

where $\theta = (\theta_1, \dots, \theta_p) \in \mathbb{R}^p$ is a set of reals coefficients. The function v is thus parametrized by the set of coefficients θ , and we write $v = v_\theta$ to stress this dependency. In what follows, it will be assumed that the basis functions are continuously differentiable on $[0, 1]$ and such that h_k and $\frac{\partial}{\partial t} h_k$ vanish at $t = 0$ and $t = 1$. For the h_k 's we took in our numerical experiments a set of B-spline functions of degree 3 using equally-spaced knots on $[0, 1]$. The choice of the number p of B-spline functions is a difficult model selection problem that is discussed in Section 3.

Then, let $t \in [0, 1]$ and for $u \in [0, 1]$ consider the following ordinary differential equation (ODE)

$$(2.1) \quad \frac{\partial}{\partial u} \psi(u, t) = v_\theta(\psi(u, t))$$

with initial condition $\psi(0, t) = t$. Then, it can be shown (see *e.g.* [Younes \(2010\)](#)) that for any $u \in [0, 1]$ the solution of the above ODE is unique and

such that

$$t \mapsto \psi_{\boldsymbol{\theta}}(u, t) = t + \int_0^u v_{\boldsymbol{\theta}}(\psi_{\boldsymbol{\theta}}(s, t)) ds$$

is a diffeomorphism of $[0, 1]$ i.e. a smooth increasing function with $\psi_{\boldsymbol{\theta}}(u, 0) = 0$ and $\psi_{\boldsymbol{\theta}}(u, 1) = 0$. Then, we denote by

$$\phi_{\boldsymbol{\theta}}(t) = \psi_{\boldsymbol{\theta}}(1, t)$$

the solution at $u = 1$ of the ODE (2.1). In this way, we finally obtain a diffeomorphism $\phi_{\boldsymbol{\theta}}$ that is parametrized by the set of coefficients $\boldsymbol{\theta} \in \mathbb{R}^p$, and that is such that $\phi_{\boldsymbol{\theta}}^{-1}(t) = \phi_{-\boldsymbol{\theta}}(t)$.

2.3. Numerical implementation. To compute the smoothed Fréchet mean (1.4), one needs to minimize the criterion (1.3). For this purpose, we use a *gradient descent algorithm* with an adaptive step to compute simultaneously J vectors $\hat{\boldsymbol{\theta}}_1, \dots, \hat{\boldsymbol{\theta}}_J$ in \mathbb{R}^p minimizing (1.3). Note that in the case of non-rigid operators, it can be shown that the mapping $\boldsymbol{\theta} \mapsto \phi_{\boldsymbol{\theta}}$ is differentiable, and an explicit formula of its gradient is given by Lemma 2.1 in [Beg et al. \(2005\)](#).

An alternative approach to register the raw data is to use the following algorithm that has been originally developed for the computation of a full Procrustean mean in planar shapes analysis. This algorithm is based on an alternative scheme between estimation of deformation operators and averaging of back-transformed curves given estimated values of the deformation parameters. In what follows, it will be referred to as the *two-steps algorithm*. To be more precise, assume that $Y_j : [0, 1] \rightarrow \mathbb{R}$ denotes a linear interpolation of the data $(Y_j^\ell)_{\ell=1}^n$. Using our notations, this algorithm consists in an initialization step $\hat{f}^{(0)} = \frac{1}{J} \sum_{j=1}^J Y_j$ that is the Euclidean mean of the raw data taken as a first reference template. Then, at iteration $1 \leq i \leq i_{\max}$, it computes for all $1 \leq j \leq J$ the estimators $\hat{\boldsymbol{\theta}}_{j,i}$ of the j -th deformation parameter as

$$\hat{\boldsymbol{\theta}}_{j,i} = \arg \min_{\boldsymbol{\theta} \in \mathbb{R}^p} \frac{1}{n} \sum_{\ell=1}^n \left(Y_j(\phi_{-\boldsymbol{\theta}_j}(t_\ell)) - \hat{f}^{(i-1)}(t_\ell) \right)^2$$

and then takes $\hat{f}^{(i)}(t) = \frac{1}{J} \sum_{j=1}^J Y_j(\phi_{-\hat{\boldsymbol{\theta}}_{j,i}}(t))$ as a new reference template. This procedure is repeated until the estimated reference template does not change. Usually the algorithm converges in a few steps. In what follows, the resulting reference template after the two-steps algorithm will be referred to as the *Iterated mean*.

2.4. *Numerical experiments to illustrate the advantages of the smoothing step.* We propose to use simulated data to compare the performances of signal averaging using either the smoothed Fréchet mean (1.4) (via a gradient descent algorithm to simultaneously compute all the $\hat{\theta}_j$'s), or the Iterated mean obtained via the two-steps algorithm described in Section 2.3. For this purpose, let us consider a set of $J = 30$ signals generated from the following deformable model using translation operators:

$$(2.2) \quad Y_j^\ell = f(t_\ell - \theta_j^*) + w_j^\ell, \quad j = 1, \dots, J, \quad \text{and} \quad \ell = 1, \dots, n,$$

with additive error terms satisfying the model

$$w_j^\ell = Z_j(t_\ell - \theta_j^*) + \sigma \varepsilon_j^\ell, \quad j = 1, \dots, J, \quad \text{and} \quad \ell = 1, \dots, n,$$

where $n = 128$, the θ_j^* 's are i.i.d. normal variables with zero mean and variance $\mu^2 = 0.004$, the ε_j^ℓ 's are i.i.d. normal variables with zero mean and variance 1, f is one the signals displayed in Figure 3(a) and Figure 3(c), and the Z_j 's are i.i.d. copies of a Gaussian process $Z : [0, 1] \rightarrow \mathbb{R}$ with zero expectation. The covariance function of Z has an exponential decay such that $R(t_\ell, t_{\ell'}) = \mathbb{E}Z(t_\ell)Z(t_{\ell'}) = \sigma^2 \phi^{|\ell - \ell'|}$ with $\phi = 0.9$. To simulate independent sample paths of Z , we use the standard circulant embedding technique, see *e.g.* Wood and Chan (1994). The signal-to-noise ratio (SNR) is the measurements is defined as

$$SNR = \frac{\sqrt{\int_0^1 (f(t) - \bar{f})^2}}{\sigma} \quad \text{with} \quad \bar{f} = \int_0^1 f(t) dt.$$

To estimate f , we compare three different estimators:

- a smoothed Fréchet mean using low-pass Fourier filtering with $\hat{\lambda}_j$ chosen by GCV for each $j = 1, \dots, J$,
- the Iterated mean computed from the raw data (without smoothing) via the two-steps algorithm,
- the Iterated mean computed from smoothed data, i.e. via the two-steps algorithm using as inputs the estimates \hat{f}_j (that have been used for the computation of the smoothed Fréchet mean) instead of the linear interpolation Y_j of the raw data. This third estimator will be referred to as the smoothed Iterated mean.

To illustrate the benefits of the smoothed Fréchet mean, we used $M = 100$ replications of model (2.2) with $J = 30$, for the two signals f displayed in Figure 3 and for various values of the SNR. For each replication $m =$

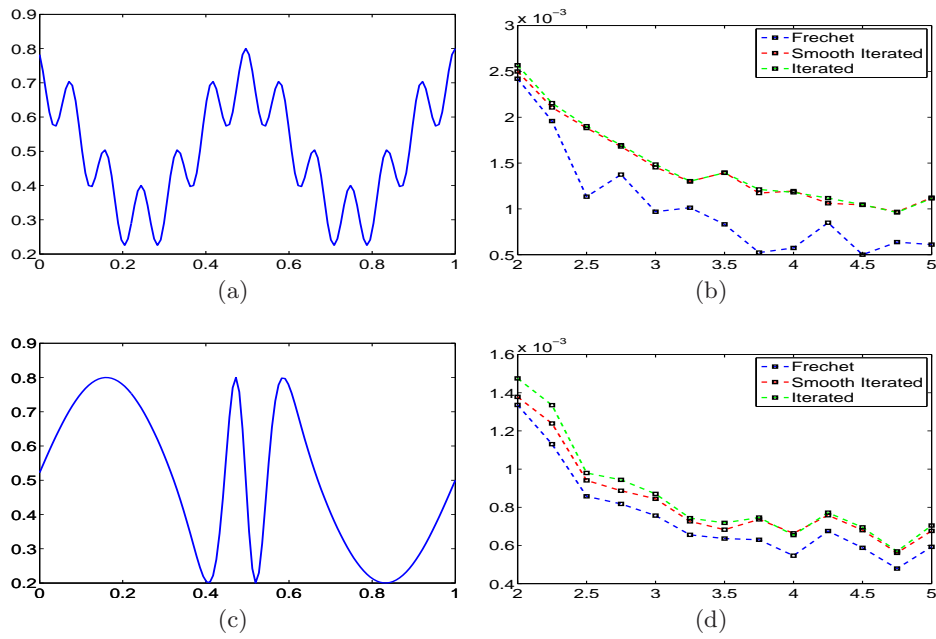


FIG 3. (a) and (c) two different test functions f ; (b) and (d) average empirical MSE ($AvMSE$) as a function of the SNR (ranging from 2 to 5) for each estimator: smoothed Fréchet mean (blue curve), smoothed Iterated mean (red curve) and Iterated mean without smoothing (green curve).

$1, \dots, M$, we compute the empirical mean squared error (MSE) at the design points of the three estimators described above. In Figure 3, we display the average value of the empirical MSE (AvMSE) over $M = 100$ repetitions as a function of the SNR. The AvMSE of the smoothed Fréchet mean is always lower than the AvMSE of the two other estimators. The smoothed Iterated mean has also a slightly lower AvMSE than the Iterated mean of the raw data without smoothing which confirms the benefits of a preliminary smoothing step before an alignment procedure.

3. Application to ECG data analysis. We now return to the analysis of the ECG record displayed in Figure 1. A smoothing of the $J = 285$ signals obtained after segmentation of the ECG record of patient Sel104 (over 4 minutes) is done by wavelet thresholding with a data-based choice of the regularization parameters $\hat{\sigma}_j$ as explained in Section 2.1. The computation of an average shape using a smoothed Fréchet mean with translation operators does not give a result that is very different from the one obtained by the Euclidean mean of the raw data. Since the activity of the heart can be very irregular in the case of cardiac arrhythmia, modeling time variability using only translation operators is not flexible enough. A more precise alignment to take into account a local variability in lag and duration of the heart beats is thus needed. Therefore, we propose to compute a smoothed Fréchet mean of these signals using the non-rigid operators given by a family of parametric diffeomorphisms parametrized by p B-spline functions, as described in Section 2.2.

Obviously, the choice of the number p of B-spline functions used to parametrize the non-rigid deformations is very important. For a given integer $p \geq 1$, let us introduce the following quantity

$$\ell_p = \frac{1}{J} \sum_{j=1}^J \frac{1}{n} \sum_{\ell=1}^n \left(\hat{f}_j(\phi_{-\hat{\theta}_j}(t_\ell)) - \frac{1}{J} \sum_{j'=1}^J \hat{f}_{j'}(\phi_{-\hat{\theta}_{j'}}(t_\ell)) \right)^2,$$

which corresponds to the minimal value of the objective function (1.3) when using non-rigid operators parametrized by a family of p B-spline functions. It is clear that one can interpret ℓ_p as a measure of mis-alignment of the data after registration. Hence, a first idea to choose an optimal value of p would be to try to minimize the value ℓ_p as a function of p to obtain the best possible alignment. In Figure 4(a), we display the curve $p \mapsto nJ\ell_p$ (for $1 \leq p \leq 20$) which is a globally decreasing function that reaches its minimal value at $p = 20$. Therefore, trying to minimize ℓ_p simply results in choosing the largest possible p .

To interpret this fact, one may remark that the quantity $nJ\ell_p$ is related to the minimal value of the negative log-likelihood of the data in the deformable model (1.1) in the case where the w_j^ℓ 's are i.i.d. normal variables with zero expectation and variance σ^2 (conditionally to the θ_j^* 's). It is widely known that increasing the number of parameters in a statistical model leads to a decay of the minimal value of the negative log-likelihood of the observed data, which explains why we observe a decay of ℓ_p as p increases in Figure 4(a). As classically done in model selection in statistics, it is thus necessary to penalize the negative log-likelihood to select an appropriate dimension of the parameters to be estimated. In Gaussian linear regression, the well-known Mallows's C_p rule Mallows (1973) suggests to penalize the negative log-likelihood by a term that is proportional to the dimension of the linear model. In our deformation model, the number of B-spline coefficients to be estimated grows linearly with p . Therefore, we propose to minimize the following penalized mis-alignment cost

$$(3.1) \quad c_p = nJ\ell_p + \beta p,$$

where $\beta > 0$ is a regularization parameter. The choice of an appropriate value for β is then motivated from general ideas in model selection proposed by Birgé and Massart (2007). Our method to find an optimal value for β (and then the corresponding optimal dimension $p = p(\beta)$), is based on the ‘‘slope heuristic’’ principle suggested in Birgé and Massart (2007). This heuristic consists in considering that the penalized cost c_p (3.1) is the sum of the negative log-likelihood that represents a data-fidelity term and the penalty term representing the complexity of the model which is related to a variance term that is generally unknown. The idea of the ‘‘slope heuristic’’ is that when a model is high-dimensional, then the associated bias is close to zero, and so the log-likelihood is essentially an estimate of the variance of the model (which we assume to be proportional to the dimension p). Hence, for large p , the negative log-likelihood should become a linear function of p . The choice of the dimension p beyond which the negative log-likelihood becomes linear is left to the user. Based on visual inspection of the curve $p \mapsto nJ\ell_p$ that is displayed in Figure 4(a), we consider that, for $p \geq 7$, the negative likelihood ceases to decrease significantly and becomes approximately linear as shown by Figure 4(b). Once we have chosen the appropriate dimension (here $p = 7$) beyond which the negative log-likelihood becomes linear, the basic principle of the ‘‘slope heuristic’’ is to fit a linear regression of $nJ\ell_p$ with respect to p for $7 \leq p \leq 20$, see Figure 4(b). If we denote by $\hat{\alpha} \approx -2,946.10^5$ the estimated regression coefficient, then as suggested by Birgé and Massart (2007), an appropriate estimator for β is $\hat{\beta} = -2\hat{\alpha} \approx 5,893.10^5$.

In Figure 4(c), we display the curve $p \mapsto \hat{c}_p = nJ\ell_p + \hat{\beta}p$ (for $1 \leq p \leq 20$). The penalized mis-alignment cost \hat{c}_p is minimal at $p = p(\hat{\beta}) = 5$ which is therefore the value that we finally choose for the statistical analysis of these ECG data.

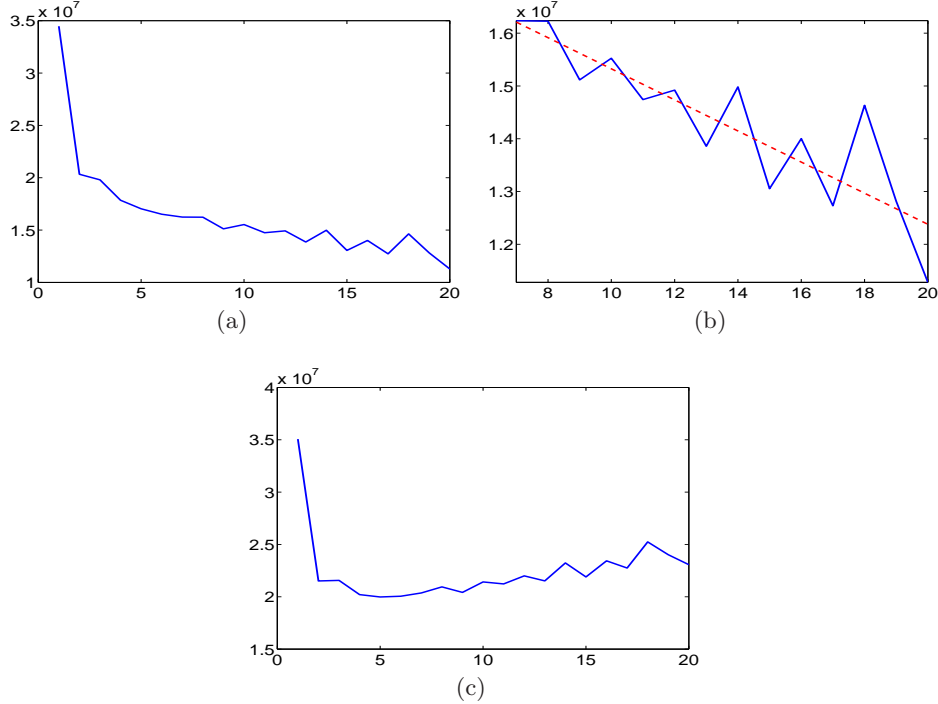


FIG 4. Patient Sel104 - (a) mis-alignment cost $nJ\ell_p$ and (c) penalized mis-alignment cost $\hat{c}_p = nJ\ell_p + \hat{\beta}p$ as functions of the dimension p ranging from 1 to 20. (b) mis-alignment cost $nJ\ell_p$ for $7 \leq p \leq 20$ (blue curve) and its approximation by an affine function (red and dashed line). The mis-alignment cost $nJ\ell_p$ is minimal at $p = 20$, while the penalized mis-alignment cost $\hat{c}_p = nJ\ell_p + \hat{\beta}p$ is minimal at $p(\hat{\beta}) = 5$.

In Figure 5, we display the smoothed Fréchet mean using the non-rigid operators parametrized by $p = 5$ B-spline functions, as described in Section 2.2. The resulting mean heart cycle in Figure 5 better reflects the typical shape of the signals than the one obtained using the Euclidean mean of the raw data that is displayed in Figure 2. In particular, there is no low-pass filtering effect around the time point $t \approx 0.45$ in the shape of this smoothed Fréchet mean.

Beyond the calculation of an average heart cycle, the computation of a

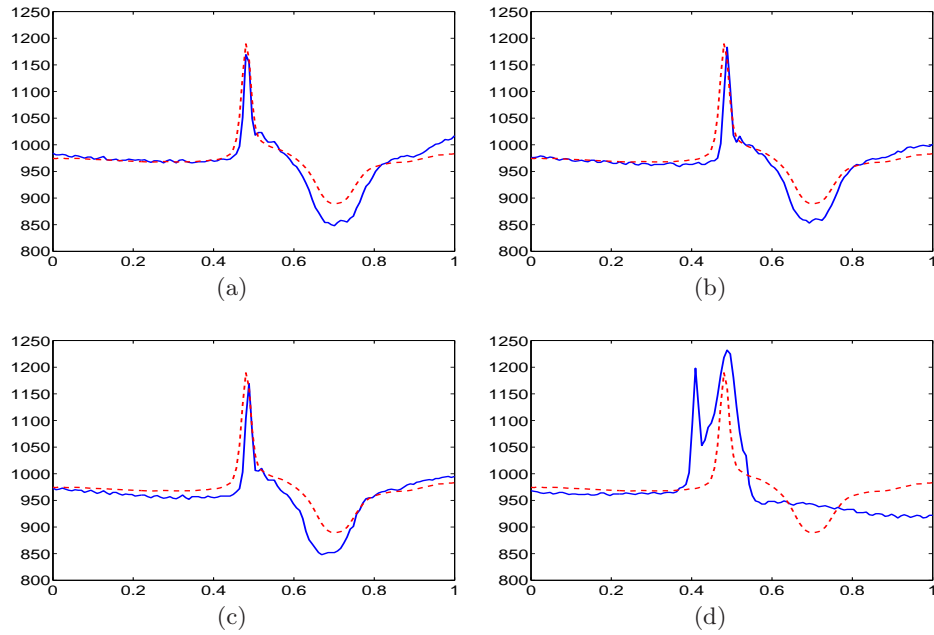


FIG 5. Patient *Sel104* - case of cardiac arrhythmia. Solid and blue curves: four signals containing a single QRS complex out of $J = 285$ extracted from the ECG recording displayed in Figure 1. The length of the signals is $n = 128$ time points. Dashed and red curve: Fréchet mean using non-rigid operators. Units on the horizontal axis are arbitrary.

Fréchet mean is also a way to separate the variability of a data set into a source of variability in time and another source of variability in amplitude (or intensity). To illustrate this point, let us first remark that the ECG record of patient Sel104 is composed of two major types of beats whose typical shapes are displayed in Figure 6(a) and in Figure 6(b). This classification of the heart beats from this ECG record in two clusters is discussed in detail in Zhou and Sedransk (2009).

In Figure 6(c), we give a two-dimensional representation of these two clusters by projecting the data on the first and second principal components (PC) of the principal components analysis (PCA) of the $J = 285$ raw signals considered as random vectors of length $n = 128$. In this representation, the sources of variability in time and in amplitude of the data are completely mixed. In particular, one cannot see if there exists more variability in lag and duration of the heart beats in one of the two clusters.

After computing the Fréchet mean of the heart beats, one can associate to each signal a set of $p = 5$ coefficients $\boldsymbol{\theta} = (\theta_1, \dots, \theta_p) \in \mathbb{R}^p$ that parametrize a non-rigid operator $\phi_{\boldsymbol{\theta}}$, see Section 2.2. These p dimensional vectors represent the variability in time of the data. In Figure 6(d), we display the projection of the data on the first and second PC of the PCA of these random vectors. This graphical representation of the data highlights two different behaviors of the signals in each cluster. The variability in time of the data of type I (red circles) is relatively low and homogeneous, contrary to the time variability of the data of type II (blue stars) that is much stronger and heterogeneous. One can also perform a PCA of the aligned and smoothed data (using these non-rigid operators). A graphical display of such a PCA is given in Figure 6(e). This further step allows to analyze the variability in amplitude in the data that is not due to a mis-alignment. It gives a different interpretation of the variability in intensity of the signals within each cluster than the one displayed in Figure 6(c) when doing a PCA of the raw data.

4. Discussion and conclusion. We have presented a new algorithm for aligning heart beats extracted from an ECG record. Our approach is based on the notion of smoothed Fréchet means of curves using deformation operators. When using non-rigid operators to align hearts beats having a high variability, with peaks showing an important variability in lag and duration from one pulse to another, our approach may be used to decompose the data into two separate sources of variation in time and in amplitude. The benefits of our procedure has been demonstrated for an ECG recording of a subject showing evidence of significant arrhythmia. Using simulated data, we have also shown the advantages of a preliminary smoothing step before

applying an alignment procedure. We hope that the methods presented in this paper will stimulate further investigation into the development of better alignment procedures that take into account time variability in heart beats extracted from ECG records.

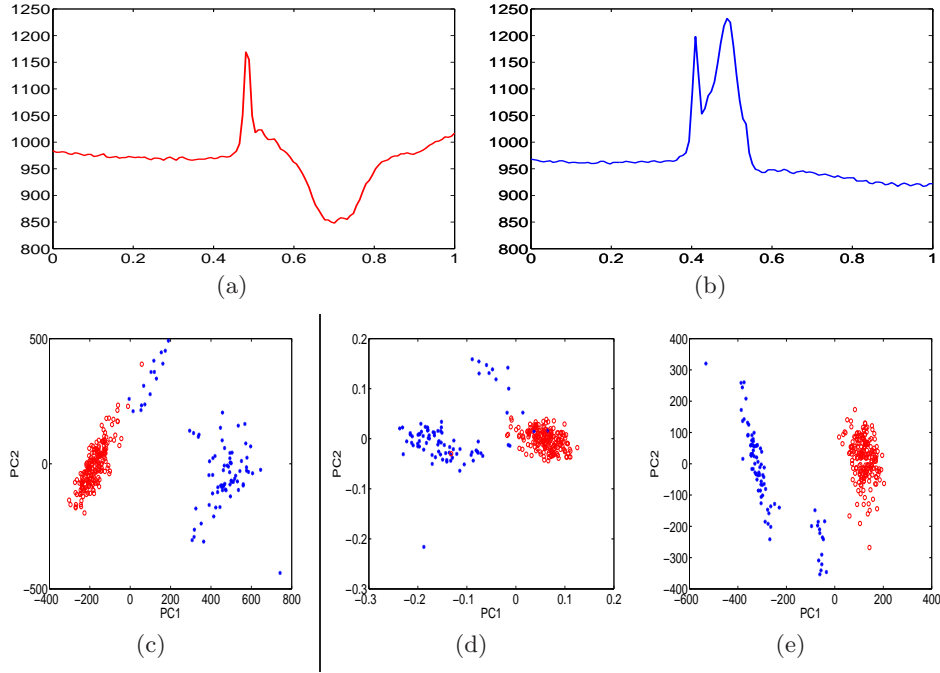


FIG 6. Patient *Sel104* - case of cardiac arrhythmia. Two types of beats (a) Type I (red curve) and (b) Type II (blue curve); (c) PCA of the raw data; (d) **Variability in time** via PCA of the coefficients of the B-splines encoding the non-rigid operators used to compute the Fréchet mean; (e) **Variability in amplitude** via PCA of the aligned and smoothed data. To visualize the results of the various PCA, the data are projected on the first and second principal components and they are labelled as type I (red circles) and type II (blue stars).

Acknowledgements. The author acknowledges the support of the French Agence Nationale de la Recherche (ANR) under reference ANR-JCJC-SIMI1 DEMOS.

References.

- AFSARI, B. (2011). Riemannian L^p center of mass: existence, uniqueness, and convexity. *Proceedings of the American Mathematical Society* **139** 655-673.

- ALLASSONNIÈRE, S., AMIT, Y. and TROUVÉ, A. (2007). Towards a coherent statistical framework for dense deformable template estimation. *J. R. Stat. Soc. Ser. B Stat. Methodol.* **69** 3–29. [MR2301497 \(2008m:62105\)](#)
- ANTONIADIS, A., BIGOT, J. and SAPATINAS, T. (2001). Wavelet Estimators in Nonparametric Regression: A Comparative Simulation Study. *Journal of Statistical Software* **6** 1–83.
- BEG, M. F., MILLER, M. I., TROUVÉ, A. and YOUNES, L. (2005). Computing Large Deformation Metric Mappings via Geodesic Flows of Diffeomorphisms. *Int. J. Comput. Vision* **61** 139–157.
- BIGOT, J. (2006). Landmark-based registration of curves via the continuous wavelet transform. *J. Comput. Graph. Statist.* **15** 542–564. [MR2291263](#)
- BIGOT, J. and CHARLIER, B. (2011). On the consistency of Fréchet means in deformable models for curve and image analysis. *Electronic Journal of Statistics* **5** 1054–1089.
- BIGOT, J., GADAT, S. and LOUBES, J. M. (2009). Statistical M-estimation and consistency in large deformable models for image warping. *J. Math. Imaging Vision* **34** 270–290. [MR2515449 \(2010h:68190\)](#)
- BIGOT, J. and GADAT, S. (2010). A deconvolution approach to estimation of a common shape in a shifted curves model. *Annals of statistics* **38** 2422–2464.
- BIGOT, J. and GENDRE, X. (2013). Minimax properties of Fréchet means of discretely sampled curves. *Annals of statistics* **41** 923–956.
- BIRGÉ, L. and MASSART, P. (2007). Minimal penalties for Gaussian model selection. *Probab. Theory Related Fields* **138**.
- CRAVEN, P. and WAHBA, G. (1979). Smoothing noisy data with spline functions: Estimating the correct degree of smoothing by the method of generalized cross-validation. *Numer. Math.* **31** 377–403.
- FLETCHER, P. T., LU, C., PIZER, S. M. and JOSHI, S. (2004). Principal geodesic analysis for the study of nonlinear statistics of shape. *IEEE TRANSACTIONS ON MEDICAL IMAGING* **23** 995–1005.
- FRÉCHET, M. (1948). Les éléments aléatoires de nature quelconque dans un espace distancié. *Ann. Inst. H. Poincaré, Sect. B, Prob. et Stat.* **10** 235–310.
- GAMBOA, F., LOUBES, J. M. and MAZA, E. (2007). Semi-parametric estimation of shifts. *Electron. J. Stat.* **1** 616–640.
- GASSER, T. and KNEIP, A. (1995). Searching for Structure in Curve Samples. *Journal of the American Statistical Association* **90** 1179–1188.
- GOLDBERGER, A. L., AMARAL, L. A. N., GLASS, L., HAUSDORFF, J. M., IVANOV, P. C., MARK, R. G., MIETUS, J. E., MOODY, G. B., PENG, C. K. and STANLEY, H. E. (2000). PhysioBank, PhysioToolkit, and PhysioNet: Components of a New Research Resource for Complex Physiologic Signals. *Circulation* **101** e215–e220.
- GOODALL, C. (1991). Procrustes methods in the statistical analysis of shape. *J. Roy. Statist. Soc. Ser. B* **53** 285–339. [MR1108330 \(92e:62113\)](#)
- GUYTON, A. C. and HALL, J. E. (2006). *Textbook of medical physiology*. Elsevier Saunders.
- HUCKEMANN, S. (2011). Intrinsic Inference on the Mean Geodesic of Planar Shapes and Tree Discrimination by Leaf Growth. *Ann. Statist.* **39** 1098–1124.
- KLASSEN, E., SRIVASTAVA, A., MIO, M. and JOSHI, S. H. (2004). Analysis of planar shapes using geodesic paths on shape spaces. *Pattern Analysis and Machine Intelligence, IEEE Transactions on* **26** 372–383.
- KNEIP, A. and GASSER, T. (1988). Convergence and consistency results for self-modelling regression. *Annals of Statistics* **16** 82–112.
- LACIAR, E., JANÉ, R. and BROOKS, D. H. (2003). Improved alignment method for noisy

- high-resolution ECG and Holter records using multiscale cross-correlation. *IEEE Trans. Biomed. Eng.* **50** 344-53.
- LIU, X. and MULLER, H. G. (2004). Functional Convex Averaging and Synchronization for Time-Warped Random Curves. *Journal of the American Statistical Association* **99** 687-699.
- MA, J., MILLER, M. I., TROUVÉ, A. and YOUNES, L. (2008). Bayesian Template Estimation in Computational Anatomy. *NeuroImage* **42** 252-261.
- MALLOWS, C. L. (1973). Some comments on Cp. *Technometrics* **15** 661-675.
- PAN, J. and TOMPKINS, W. J. (1985). A real-time QRS detection algorithm. *IEEE Trans Biomed Eng* **32** 230-236.
- RAMSAY, J. O. and LI, X. (2001). Curve Registration. *Journal of the Royal Statistical Society (B)* **63** 243-259.
- ROMPELMAN, O. and ROS, H. H. (1986a). Coherent averaging technique: a tutorial review. Part 1: Noise reduction and the equivalent filter. *J. Biomed. Eng.* **8** 24-9.
- ROMPELMAN, O. and ROS, H. H. (1986b). Coherent averaging technique: a tutorial review. Part 2: Trigger jitter, overlapping responses and non-periodic stimulation. *J Biomed Eng* **8** 30-5.
- TRIGANO, T., ISSERLES, U. and RITOV, Y. (2011). Semiparametric Curve Alignment and Shift Density Estimation for Biological Data. *IEEE Transactions on Signal Processing* **59** 1970-1984.
- VIMOND, M. (2010). Efficient estimation for a subclass of shape invariant models. *Annals of statistics* **38** 1885-1912.
- WANG, K. and GASSER, T. (1997). Alignment of Curves by Dynamic Time Warping. *Annals of Statistics* **25** 1251-1276.
- WOOD, A. T. A. and CHAN, G. (1994). Simulation of stationary Gaussian processes in $[0, 1]^d$. *J. Comput. Graph. Statist.* **3** 409-432.
- YOUNES, L. (2010). *Shapes and diffeomorphisms*. *Applied Mathematical Sciences* **171**. Springer-Verlag, Berlin. [MR2656312](#)
- ZHOU, Y. and SEDRANSK, N. (2009). Functional data analytic approach of modeling ECG T-wave shape to measure cardiovascular behavior. *Ann. Appl. Stat.* **3** 1382-1402.

DÉPARTEMENT MATHÉMATIQUES, INFORMATIQUE, AUTOMATIQUE (DMIA)
 INSTITUT SUPÉRIEUR DE L'AÉRONAUTIQUE ET DE L'ESPACE (ISAE)
 10, AVENUE ÉDOUARD-BELIN
 BP 54032 - 31055 TOULOUSE CEDEX 4, FRANCE.
 E-MAIL: Jeremie.Bigot@isae.fr